

JSACE 2/15

Microstructure and
Aging Influence
on the Mechanical
Properties of High-
Voltage Poles

Received
2016/08/19

Accepted after
revision
2016/09/29

Microstructure and Aging Influence on the Mechanical Properties of High-Voltage Poles

Jūratė Mockienė*

Department of Building Structures, Kaunas University of Technology
Studentu str. 48, LT- 51367 Kaunas, Lithuania

Audrius Jutas

Department of Mechanical Engineering, Kaunas University of Technology
Studentu str.56, LT- 51424 Kaunas, Lithuania

Vilimantas Vaičiukynas

Faculty of Water and Land Management, Aleksandras Stulginskis University
Universiteto g.10, LT-53361 Akademija, Kaunas District Municipality, Lithuania

*Corresponding author: jurate.mockiene@ktu.lt

 <http://dx.doi.org/10.5755/j01.sace.15.2.16092>

High-voltage poles made in 1956 had to satisfy the cross-sectional geometry related standard (GOST 8509-57 confirmed later). However, the stricter requirements weren't applied for the microstructure. In this paper a strength analysis of the pillars' material is provided. The technological specificities of profile manufacturing were mostly determined by differences in mechanical properties influenced by differences in microstructures of pillars' material investigated. Although the confirmed standard of steel CT3 (GOST 380-71) had new requirements and clear criteria of microstructure acceptance but made pillars with the non-homogeneous microstructure remained standing. The differences in microstructural components create conditions for appreciable differences in mechanical properties such like yield stress and ultimate stress, fracture strain. In this paper, the limits of elastic and plastic strains are identified in order to quantify the changes in elastic and plastic properties with the differences in their intensity for selected step-like stress range. Corrosion depth and width play the large role and ones often determine the fracture location of samples. The end of this work is dedicated to conclusion based on the relation of experimental part and analytical calculations presented.

KEYWORDS: ageing, corrosion, microstructure, mechanical properties.

Introduction

The tensile properties of the alloys have been measured at room temperature as an expected function of corrosion level. Investigation indicates that the very fine stable microstructure of the specimens' material influences on mechanical properties combined with adequate corrosion impact. Corrosion evolution on the cold-rolled low carbon steels is one of many examples of dynamics in corrosion that may occur under atmospheric/oxidizing conditions. Cold forming operations and cold rolling generally do not decrease the corrosion resistance (Barbier *et al.* 2009). It is important that such kind of steels do not demonstrate sufficient resistance to the corrosive effects of the most commonly encountered environment like atmosphere.

In this article, authors present their study how level of corrosion may influence on mechanical properties after some period of maintenance time of high voltage piles. In electric industry, the



structures mentioned retain wide appearance of corrosion not only for long but also for short periods of time. Data of this investigation was analyzed statistically, and a set of equations was derived that allows comparison of corrosion level as a function of the mechanical properties presented below (Flower and Lindley 2000).

The height and roughness of exposed corrosion samples have been measured by mechanical profilometer for comparison with the results of fracture area gotten after tensile experiment. In some experimental studies, the averaged magnitude of corroded area has been used to image and map the corrosion under specimen surface and some authors showed that corrosion level may be described by the power function which is also suitable for demonstrating the development of long-term corrosion. (Garcia *et al.* 2003).

The mechanical properties and microstructures of low-carbon steel were investigated by tensile testing machine and optical microscopy, respectively. The results showed that significant differences existed in the yield strength, ultimate strength and fracture strength (Arafin and Szpunar 2009).

The aim of the present work is to show the difference in mechanical properties for cold-rolled specimen made of low carbon steel and used in old design of high-voltage poles. The differences in microstructure and corrosion related damages influence on the dissipation of mechanical properties. Used statistical method shows how experimental results are close to their mean values and what reasons of microstructural quality lead to those differences (Serenelli *et al.* 2011, Hughes *et al.* 2003).

The present work is important for the development of statistical method that tries to overcome details of the differences in microstructure and level of corrosion on the specimen surface as a result of deformational state of material. The microstructural observations show that the difference of material quality naming it as a non-homogeneous specimen has a significant effect on different stages of deformation. The description of mechanical behaviour of crystalline material is a complex multiscale problem. While the underlying deformation processes such as the intergranular slip lead atomic plane inclinations and like-screw dislocations are microscopic problems, the measured results exhibit usually macroscopic stages. As it is presented in this work, provided tensile tests show a deformational behaviour of individual specimens. They also may exhibit that some level of corrosion over the area of the specimen is the reason of fracture.

Tensile test were provided using the standard LST EN ISO 6892-1:2009. The standard exhibits basic requirements for the methodology of test procedure like specimen geometry and speed of straining. During the test authors use deformation speed 1 mm/min. The result of the tests especially is important for an assessment of differences in deformational behaviour and it is one of the principal criteria of material quality of specimen.

The principal mechanical properties were fixed using experimental curve “force vs. displacement” and calculated for individual specimens separately to find means presented in Table 1.

Kind of stress/ strain	Stresses, MPa		Strains, %	
	i	ii	iii	iv
A	300.6	300.6	0.4	0.4
B	429.3	573.2	9.1	32
C	354.9	669.9	12.2	71.2

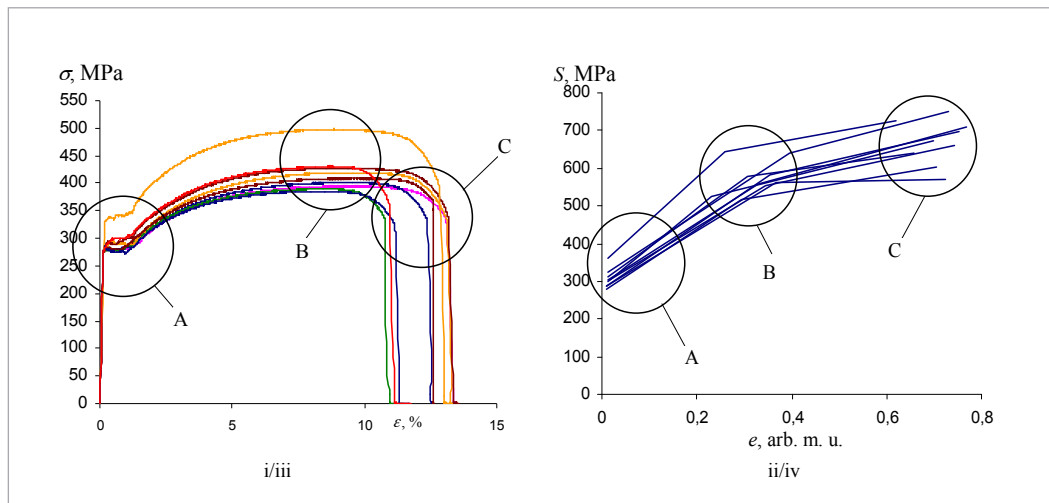
Methods

Table 1

Principal mechanical properties for family of tensile curves; averaged (see Fig. 1)

Fig. 1

Family of tensile curves in terms of engineering (i/iii) and true (ii/iv) stresses/strains, respectively. Explanation of stress/strain state related letters: A is yielding, B is ultimate, C is fracture



For the statistical analysis, authors try to choose some alternative method on approximation of results and it is necessary to determine the values of the probability distribution over the variable experimental values changing their interval. It also influences on determination of the type of data distribution. In most cases the data are distributed according to the normal (Gaussian) law.

Using hypothetical assumptions in statistical calculations, it is important to have some sufficient number of specimens. In the case of small number of specimens, there are some problems related usually with data normality. Then, description or approximation of results is difficult. In determining the distribution type, authors assume that the data may be distributed by the normal distribution. Normal distribution was defined by the arithmetic mean X_{ave} of mechanical properties and statistical analysis of their distributed values X_i for some specimens' set. Therefore, in further analysis authors try to use that assumption of normal law and used criteria will provide some quality of analysis. The literature indicates that a rough estimation of the distribution determination is sufficient if number of experiments is at least 20. In our study there were 9 specimens tested.

The individual statistical values X_i are dissipated around the arithmetic mean value X_{ave} or around relative mean value $\bar{X} = 1$ with some probabilistic value Δ and ones represent some density of points influencing on data normality. Authors use simplified method how to visualize such kind of distribution by the equation

$$\Delta \left(\begin{array}{l} \bar{X}_j < 1 \\ \bar{X}_j > 1 \end{array} \right) = \left(1 \mp \left| 1 - \frac{X_i}{X_{ave}} \right| \right) \times 100\% = \left(1 \mp |\bar{X} - \bar{X}_i| \right) \times 100\% \quad (1)$$

where $\bar{X}_i = \frac{X_i}{X_{ave}}$; $X_{ave} = \frac{1}{n} \sum_{i=1}^n X_i$; X_i is mechanical property related value of individual specimen

used; $i = 1 \dots 9$.

For the approximation of expected statistical distribution of experimental results, following equation was used:

$$\bar{Y} = C_1 \bar{X}^n + C_2 \bar{X}^{n-1} + C_3 \bar{X}^{n-2} + \dots + C_m \bar{X}^{n-m} + C_n \bar{X}^{n-m-1}; \text{ if } m = n-1. \quad (2)$$

The parameter Δ ($\Delta = \bar{Y}$) was adopted to determine some expectation related probability of mechanical property that reaches maximal value at point $\bar{X} = 1$. The final equation was chosen according to the maximal value of squared root deviation R^2 for stresses and for strains, respectively, presented in the Tables 2 and 3.

In terms of stresses and strains, Eq. 1 may be written as follows

$$\Delta_{\sigma} \begin{pmatrix} \bar{X}_{\sigma} < 1 \\ \bar{X}_{\sigma} > 1 \end{pmatrix} = \left(1 \mp \left| 1 - \frac{X_{\sigma i}}{X_{\sigma(ave)}} \right| \right) \times 100\% = (1 \mp |\bar{X}_{\sigma} - \bar{X}_{\sigma i}|) \times 100\% \quad (3)$$

and Eq. (2) adopted for stress looks like

$$\Delta_{\sigma} = C_1 \bar{X}_{\sigma}^3 + C_2 \bar{X}_{\sigma}^2 + C_3 \bar{X}_{\sigma} + C_4. \quad (4)$$

In Table 2 there are constants C_i presented according to relative mechanical property \bar{X}_{σ} with the use of third order polynomial equations Eq. (4).

X_{σ} \ C_i	C_1	C_2	C_3	C_4	R^2
A(i)	8.139	-6.212	28.000	-9.828	0.9816
B(i)	0*	-0.832	1.676	-0.745	0.9824
C(i)	0*	-0.832	1.676	-0.745	0.9824
A(ii)	8.139	-26.212	28.000	-9.828	0.9816
B(ii)	2.862	-9.583	10.574	3.754	0.9735
C(ii)	2.808	-9.373	10.309	-3.647	0.9409

Table 2

Relative mechanical properties \bar{X}_{σ} and constants C_i ($\times 10^3$) used in Eq. 4

*-Eq. 4 is transformed to second order equation

In terms of stresses and strains, Eq. 1 may be written as follows

$$\Delta_{\varepsilon} \begin{pmatrix} \bar{X}_{\varepsilon} < 1 \\ \bar{X}_{\varepsilon} > 1 \end{pmatrix} = \left(1 \mp \left| 1 - \frac{X_{\varepsilon i}}{X_{\varepsilon(ave)}} \right| \right) \times 100\% = (1 \mp |\bar{X}_{\varepsilon} - \bar{X}_{\varepsilon i}|) \times 100\%. \quad (5)$$

and Eq. (2) applied for strains is similar with Eq. (4) used for stresses:

$$\Delta_{\varepsilon} = C_1 \bar{X}_{\varepsilon}^3 + C_2 \bar{X}_{\varepsilon}^2 + C_3 \bar{X}_{\varepsilon} + C_4. \quad (6)$$

In Table 3, there are constants C_i presented according to relative mechanical property \bar{X}_{ε} with the use of same structure polynomial equations Eq. (6).

Table 3

Mechanical properties \bar{X}_ε
and constants C_i ($\times 10^3$)
used in Eq. 6

X_ε \ C_i	C_1	C_2	C_3	C_4	R^2
A(iii)	0.109	-0.520	0.703	-0.199	0.938
B(iii)	3.389	-11.331	12.488	-4.448	0.9435
C(iii)	-2.357	6.033	-4.993	1.415	0.9678
A(iv)	0.109	-0.075	0.422	-0.161	0.938
B(iv)	-0.091	-0.075	0.422	-0.161	0.937
C(iv)	-2.436	6.317	-5.321	1.539	0.9529

Using equations 3 and 5 the values Δ_σ and Δ_ε were obtained and ones represent dots in the plotted graph of Fig. 2. For those dots distributed around the relative mean $\bar{X}=1$ in the left and right sides the equations of approximation Eq. 5 and Eq. 6 were applied.

In Fig. 2, i(a) the mostly dissipated engineering stress is stress B with its value $\bar{X}_\sigma = 1.18$ and $\Delta_\sigma = 82\%$. Also, for same enlarged distribution presented in Fig. 2, i(b) the picks of engineering stress on the dashed mean line $\bar{X}=1$ represents maximal values of that distribution related characteristics A, B and C. Obviously, for A - $\Delta_\sigma(\max) = 99\%$, for B - $\Delta_\sigma(\max) = 98.5\%$ and for C - $\Delta_\sigma(\max) = 98\%$.

In the case of true stress (see Fig. 2, ii(a)), the characteristics A and C are dissipating mostly with the values $\bar{X}_\sigma = 1.15$, $\Delta_\sigma = 85\%$ and $\bar{X}_\sigma = 0.85$, $\Delta_\sigma = 85\%$, respectively. Enlarged view (Fig. 2, ii(b)) shows approximately same values for Δ_σ in comparison with engineering stress mentioned above but dots are dissipated widely along to axis \bar{X}_σ . This fact is related to the differences in methods for stresses used non-/reducing area of cross-section.

In Fig. 2. graphs iii and iv exhibit families of engineering and true strains, respectively. The largest difference was gotten for curve A representing engineering yield strain at the highest pick of yield stress σ_Y (Fig. 2, iii(a)). The dissipation was high enough $\bar{X}_\varepsilon = 1.6$ and its probability was very low $\Delta_\varepsilon = 36\%$. In the shorter enlarged range (Fig. 2, iii(b)), the picks reach following values: for A - $\Delta_\varepsilon(\max) = 92.5\%$ but $\bar{X}_\varepsilon = 0.97$, for B and C - $\Delta_\varepsilon(\max) = 98.5\%$.

True strain curves show similar distribution of mechanical characteristics A, B and C but the points in the curves B and C are dissipated widely along to axis \bar{X}_ε (Fig. 2, iv(a)). In the case of true strains, the contraction of cross-section area changes pick of characteristic B with value $\Delta_\varepsilon(\max) = 95.5\%$ while it was higher for engineering strain $\Delta_\varepsilon(\max) = 98.5\%$.

Results

To describe the effects during deformation within the microstructure caused by heterogeneity is difficult because of disorientation of atomic planes in the crystals. Such analyses have difficulty accounting for the evolution of yield surfaces in the crystals that are first sources of plastic deformation. These effects were not taken into account but they were assumed naturally occurring as inevitable process.

The microstructural heterogeneity is usually inherited from the crystallization if the carbon amount in the edge and in

the centre of steel ingot is different. Iron oxides influence on the mechanical properties much stronger because of the joining fireplaces of those oxides inside the material. In the case of large amount of oxides, those fireplaces can easily connect by themselves and give a star to an earlier material degradation. The oxides especially are dangerous if their amounts are distributed stochastically inside the microstructure.

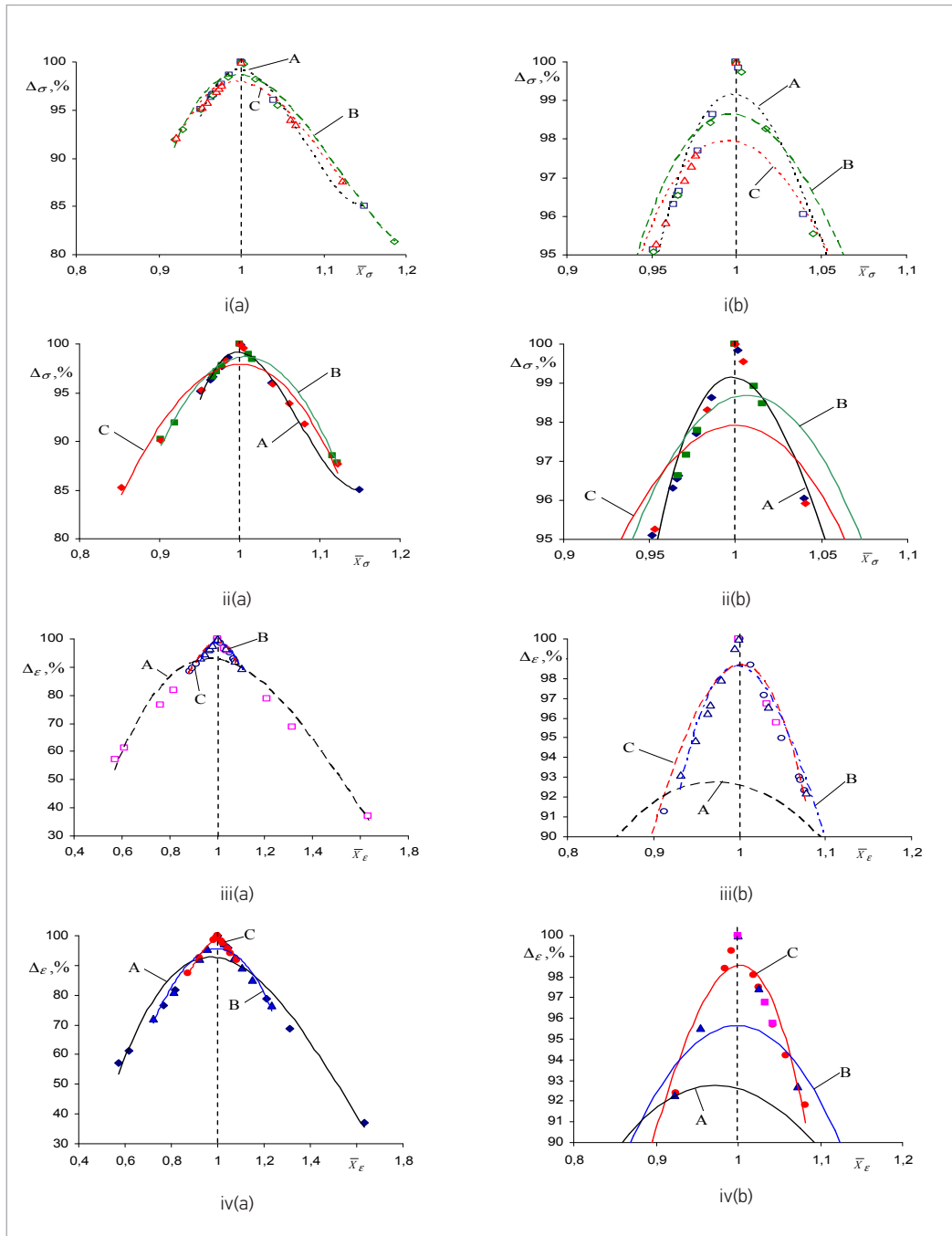


Fig. 2

Parameters representing statistical distribution of relative stresses \bar{x}_σ and strains \bar{x}_ϵ versus related probabilistic values Δ_σ and Δ_ϵ , respectively. Explanation of letters used: i and ii are engineering and true stresses; iii and iv are engineering and true strains; (a) is full set of results and (b) is enlarged view for chosen bi-axial range of figure (a)

After examination of the fracture photos the irregular damage of material along the tested samples which surface affected by long-term corrosion was revealed. As a result the characteristic parameters of corrosion defects were determined: such as the corrosion level, the approximate area of the damage, the intensity of corrosion and so on. On the surface of observed samples corrosion damage area and volume increase was examined according to the regulations of Europe standard for metal and alloy corrosion and so on (LST EN ISO 8403:2000).

$$R = 3(2 - \log_{10} A) \quad (7)$$

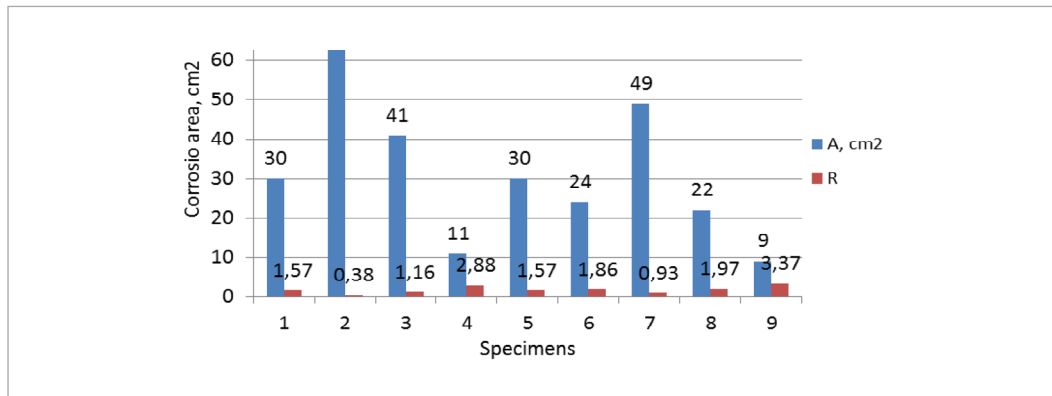
where:

R is the estimate of corrosion on any surface (area);

A is the relative area of any surface coated with corrosion defects.

Fig. 3

The diagram of corrosion area (A, cm²) influencing on indicator of corrosion affects R. Notes: 1-9 are numbers of specimens



Data of this investigation presented in Fig. 3. The study found the dispersion of corrosion spots and the differences of intensity damage (cracks) on the sample surface or the surface layer. By using the Photoshop program the rust area of ten samples was calculated. In calculating area, the program self-identified rusty color intensity of its surface area. Then this program calculated the area of pixels, and later pixels was converted into area units (cm²) according the known area.

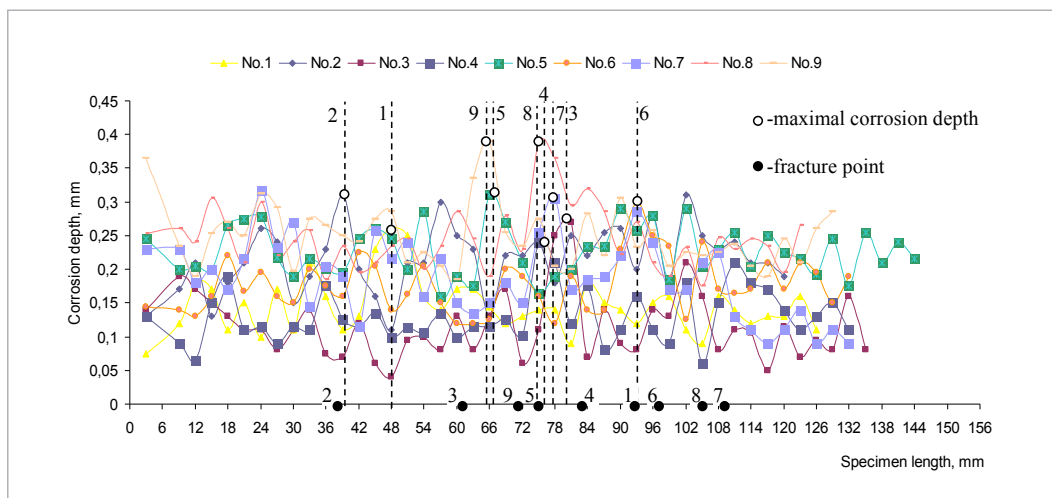
The area of rust was calculated on ten samples by choosing the rustiest spots of investigated samples. The study found that the rusty area of individual samples varied in the range of 0.26 cm² to 3.06 cm² (Fig. 3). The area of average rusty was 1.24 cm², or 31% calculating from the measured area. By identifying rust damage spot the cleaning of sample surface could be affected on the size of dispersion.

All samples have similar microstructure like steel CT 3 (GOST). Many of the studied samples are microstructurally inhomogeneous, that is, in the microstructure there were found areas with a lower carbon amount of about 0.1% C, and areas with a higher carbon amount reaching 0.3% C. Those inaccuracies were the primary sources of material fracture presenting in Fig. 4. Samples containing more homogeneous microstructure had quantity of carbon equal to 0.14–0.22%. It is obvious looking at microstructures presented in Fig. 5.

Correlation between depth of corrosion and area of fracture is weak enough as it is shown in Fig. 5. In the microstructures, there is some amount of other kind of defects like non-metallic inclusions (iron oxides and sulphides, decarbonizes surface layer, bandwidth and “Widmanstatten” pattern).

Fig. 4

The curves showing how a maximal depth of corrosion measured influences on the fracture point along to individual specimen length under tensile test



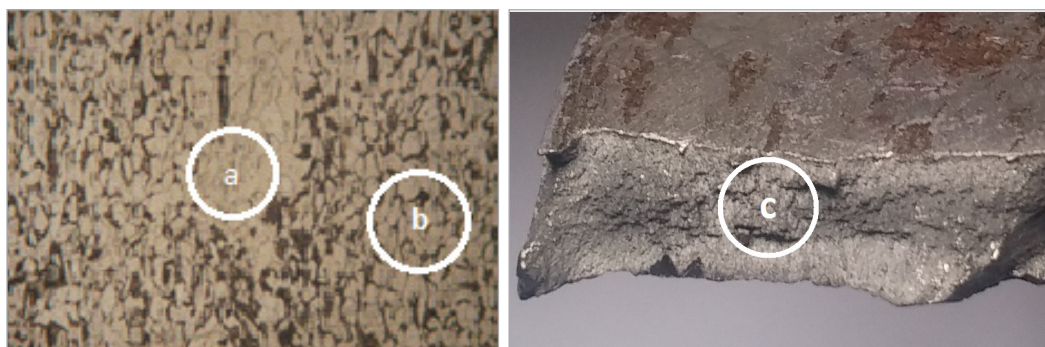


Fig. 5

Pictures representing differences in microstructure and phenomena in the area of fracture, material CT3 (GOST 380-71): a – homogeneous microstructure; b – non-homogeneous microstructure; c – area of fracture

Non-metallic inclusions are inserted themselves in all samples as both oxides and sulphides. Plastic sulphides are not seen in all samples. The negative effects are usually manifested in those cases if they are located in the transverse direction of the load. In the rolled profiles, these inclusions are parallel to the rolling direction. The influence of sulphides' amount distributed along to rolling direction on the mechanical properties is weak.

According to research it was conducted that the rusty area of individual samples varied in the range from 0.26 cm² until 3.06 cm² and the area of average rusty 1.24 cm² was or 31%, calculating from the measured area. Investigation shows that differences in microstructure caused by differences in its homogeneity were the primary reason of material fracture. In the tested steel samples the microstructure was typical for steel CT 3 (GOST), but many of the analyzed samples were non-homogeneous microstructurally: C content varied from 0.1% to 0.3%. It was likely that this non-homogeneity were the primary reason for the material fracture. Such qualitative differences and imperfections create conditions for the strain instability appearing due to deformation showing wide distribution around relative means $\bar{X}_{\sigma} = 1$ and $\bar{X}_{\epsilon} = 1$.

Conclusions

Arafin, M. A., & Szpunar, J. A. 2009. A new understanding of intergranular stress corrosion cracking resistance of pipeline steel through grain boundary character and crystallographic texture studies. *Corrosion Science*, 51(1), 119-128. <http://dx.doi.org/10.1016/j.corsci.2008.10.006>

Barbier, D., Gey, N., Allain, S., Bozzolo, N., & Humbert, M. 2009. Analysis of the tensile behavior of a TWIP steel based on the texture and microstructure evolutions. *Materials Science and Engineering: A*, 500(1), 196-206. <http://dx.doi.org/10.1016/j.msea.2008.09.031>

Flower, H. M., & Lindley, T. C. 2000. Electron back-scattering diffraction study of acicular ferrite, bainite, and martensite steel microstructures. *Materials Science and Technology*, 16(1), 26-40. <http://dx.doi.org/10.1179/026708300773002636>

García, I., Conde, A., Langelaan, G., Franssaer, J., & Celis, J. P. 2003. Improved corrosion resistance

through microstructural modifications induced by codepositing SiC-particles with electrolytic nickel. *Corrosion Science*, 45(6), 1173-1189. [http://dx.doi.org/10.1016/S0010-938X\(02\)00220-2](http://dx.doi.org/10.1016/S0010-938X(02)00220-2)

Hughes, D.A., Hansen, N., D.J. Bammann, D.J. 2003. Geometrically necessary boundaries, incidental dislocation boundaries and geometrically necessary dislocations, *Scripta Materialia*, 48, pp. 147-153. [http://dx.doi.org/10.1016/S1359-6462\(02\)00358-5](http://dx.doi.org/10.1016/S1359-6462(02)00358-5)

LST EN ISO 8403:2000. Metallic coatings. Coatings anodic to the substrate. Rating of test specimens subjected to corrosion tests.

Serenelli, M.J., Bertinetti, M.A., J.W. Signorelli, J.W. 2011. Study of limit strains for FCC and BCC sheet metal using polycrystal plasticity *International Journal of Solids and Structures*, 48, pp. 1109-1119. <http://dx.doi.org/10.1016/j.ijlsolstr.2010.12.013>

References

About the authors

JŪRATĖ MOCKIENĖ

Master degree, Lektor

Department of Building Structures, Kaunas University of Technology.

Research interests

Steel structures, strength, durability, destruction, rational design.

Address

Kaunas University of Technology,
Studentu st.48, LT- 51367
Kaunas, Lithuania.
Tel.+37068227397
E-mail: jurate.mockiene@ktu.lt

AUDRIUS JUTAS

Dr., Associate Professor

Department of Mechanical Engineering, Kaunas University of Technology.

Research interests

Accident expertise, mechanics of materials, strength of materials, strength of structural elements

Address

Kaunas University of Technology,
Studentų st.56, LT- 51424 Kaunas,
Lithuania.
Tel.+37068378880
E-mail: audrius.jutas@ktu.lt

VILIMANTAS VAIČIUKYNAS

Dr., Lektor

Institute of Water Resources Engineering, Aleksandras Stulginskis University.

Research interest

Constructions of hydrotechnical structures, drainage materials, urban hydrology.

Address

Universiteto g.10, LT- 53361
Akademija
Tel. +37061434230
E-mail: vilimantas.vaiciukynas@asu.lt